

1 **Intrinsic variability of fluorescence calibrators impacts the**
2 **assignment of MESF or ERF values to nanoparticles and extracellular**
3 **vesicles by flow cytometry**

4
5 **Estefanía Lozano-Andrés^{1, #}, Tina Van Den Broeck^{2, #}, Lili Wang³, Majid Mehrpouyan⁴, Ye**
6 **Tian⁵, Xiaomei Yan⁵, Marca H.M. Wauben^{*1, #}, Ger. J.A. Arkesteijn^{*1}**

7 1 Department of Biomolecular Health Sciences, Faculty of Veterinary Medicine, Utrecht
8 University, Utrecht, The Netherlands

9 2 BD Biosciences, Erembodegem, Belgium

10 3 Biosystems and Biomaterials Division, National Institutes of Standards and Technology (NIST),
11 Gaithersburg, MD 20899

12 4 BD Biosciences, San Jose, CA 95131

13 5 Department of Chemical Biology, MOE Key Laboratory of Spectrochemical Analysis &
14 Instrumentation, Key Laboratory for Chemical Biology of Fujian Province, College of Chemistry
15 and Chemical Engineering, Xiamen University, Xiamen 361005, People's Republic of China

16 # TRAIN-EV Marie Skłodowska-Curie Action-Innovative Training Network, train-ev.eu

17 *Both authors contributed equally

18

19 **Corresponding author:**

20 Marca H.M. Wauben

21 Department of Biomolecular Health Sciences

22 Faculty of Veterinary Sciences

23 Utrecht University
24 Yalelaan 2, 3584 CM
25 Utrecht, The Netherlands
26 T: +31 30 2535451
27 E: m.h.m.wauben@uu.nl

28

29 **Abstract**

30 Flow cytometry is commonly used to characterize nanoparticles (NPs) and extracellular vesicles
31 (EVs) but results are often expressed in arbitrary units to indicate fluorescence intensity. This
32 hampers interlaboratory and inter-platform comparisons. We investigated the use of molecules of
33 equivalent soluble fluorophores (MESF)-beads for assignment of fluorescence values to NPs and
34 EVs by comparing two FITC-MESF bead sets as calibrators on different flow cytometry platforms
35 (BD Influx™, CytoFLEX LX™ and SORP BD FACSCelesta™). Next, fluorescence signals of
36 NPs and EVs were calibrated using different sets of FITC and PE-MESF beads. Fluorescence
37 calibration using beads designed for cellular flow cytometry allowed inter-platform comparison.
38 However, the intrinsic uncertainty in the fluorescence assignment to these MESF beads impacts
39 the reliable assignment of MESF values to NPs and EVs based on extrapolation into the dim
40 fluorescence range. Our findings demonstrate that the use of the same set of calibration materials
41 (vendor and lot number) and the same number of calibration points, greatly improves robust
42 interlaboratory and inter-platform comparison of fluorescent submicron sized particles.

43 **Key words:** fluorescence, calibration, standardization, MESF, extracellular vesicles,
44 nanoparticles, flow cytometry

45

46

47 **Introduction**

48 A well-known fluorescence calibration method in flow cytometry (FC) is the use of fluorescent
49 beads to which a measurement value is assigned using standardized units established by the
50 National Institute of Standards and Technology (NIST), such as molecules of equivalent soluble
51 fluorophores (MESF) or equivalent number of reference fluorophore (ERF). This calibration
52 method was developed for cellular FC and allows for quantifiable fluorescence measurements and
53 platform comparison. The fluorescence intensity on the calibrator beads matches the expected
54 intensity on the labeled cells. Therefore, the calibrated cellular fluorescence variation closely
55 compares to the intrinsic variation on the calibrator and allows for data interpolation [1-4]. In 2012,
56 a NIST/ISAC standardization study reported differences in the assigned units to calibrators from
57 different manufactures, indicating the importance of the examination of the accuracy and precision
58 of available calibrators [5]. Nevertheless, the assignment of a specific MESF or ERF value to
59 calibration beads is inextricably bound to a variation around this value. This variation translates in
60 an uncertainty level between the measured and the assigned values that remains acceptable as long
61 as the sample values are within the range of the calibrator.

62 During the last decade, small particle FC has become a powerful tool for high-throughput analysis
63 of nanoparticles (NPs) and cell-derived extracellular vesicles (EVs) [6, 7]. However, EV
64 measurements are challenging, mainly because the vast majority of EVs is small in size (<200nm)
65 and their light scattering and fluorescent signals are typically close to, at, or below the instrument's
66 detection limit [8]. Furthermore, the majority of data is reported in arbitrary units of fluorescence,
67 which is cumbersome for the analysis of dim and small particles, whereby particles cannot be fully
68 discriminated from negative counterparts and background signals. The MIFlowCyt-EV framework
69 recommends the use of MESF beads for calibration and standardized reporting of EV flow
70 cytometric experiments, especially when a fluorescent threshold is applied [8]. However, since

71 available calibrators are developed for cells and as such are much brighter in fluorescence than
72 EVs it is unknown to which extent these calibrators will provide precision and/or accuracy for the
73 assignment of fluorescent values to NPs and EVs. We investigated how the given units of the
74 calibrator impact the regression line for assignment of MESF and/or ERF units to NPs and EVs.
75 Therefore, we evaluated custom-made calibrator beads sets from the same manufacturer on three
76 different flow cytometers and provide insights on how different bead sets affect the calibration of
77 fluorescence signals from NPs and EVs.

78

79 **Results**

80 **Assessment of precision and accuracy of different MESF bead sets for fluorescence** 81 **calibration across platforms**

82 To assess the precision and accuracy of MESF bead sets for fluorescence calibration across
83 platforms, two FITC MESF bead sets of 6 μm and 2 μm , containing respectively five or four
84 fluorescent bead populations, were selected for measurements on three different instruments,
85 namely a BD Influx, a BC CytoFLEX and a SORP BD FACSCelesta™. Since calibrator bead
86 sets can differ in the number of fluorescent bead populations (typically ranging from 3 to 5) and
87 the number of calibrator points can impact the slope of the regression line (Figure S1a-b), we
88 included for fluorescence calibration across platforms equal numbers of fluorescent bead
89 populations ($n=4$) of the two FITC MESF bead sets that were consistently measured on all three
90 platforms (Figure 1).

91 Singlet gated populations are displayed as overlays in histograms showing the FITC fluorescence
92 (Figure 1a) and indicated from dim to bright as p1, p2, p3 and p4 (Figure 1b). The 6 μm FITC
93 MESF beads contained overall brighter fluorescent intensities, whose assigned values range from
94 25,910 to 715,225 FITC MESF, while the 2 μm FITC MESF beads covered a dimmer part of the

95 fluorescence intensity range with assigned values ranging from 3,634 to 103,706 FITC MESF.
96 Clearly, MFI arbitrary units cannot be directly compared between instruments (Figure 1b), but after
97 fluorescence calibration comparable FITC MESF units could be assigned (Figure 1c-d).
98 Nevertheless, the two calibration bead sets displayed a different slope with a consistent tendency
99 across the three platforms, suggesting a variation introduced by an inherent attribute of the beads
100 themselves. This lead us to further examine the robustness of the calibration. To gain insight into
101 the precision and accuracy of MESF assignments we selected specific bead populations from one
102 set, referred to as 'unknown' in Figure 1d, to recalculate their FITC MESF units using the
103 regression line from the other bead set. The selected 'unknown' samples used were: (i) p1 and p4
104 of the 2 μm bead set for which the FITC MESF values were calculated using the regression line of
105 the 6 μm bead set and (ii) p1 and p2 of the 6 μm bead set for which the FITC MESF values were
106 calculated using the regression line of the 2 μm bead set (Figure 1c). Using this approach, the
107 calculated MESF values of p4 from the 2 μm beads and p2 from the 6 μm beads showed less than
108 20% variation (10% above or 10% below actual values) of the actual value, while data were precise
109 when compared between platforms (Figure 1d). Also the MESF values of the dimmest p1 2 μm
110 and 6 μm beads, calculated using respectively the regression lines of the 6 μm and 2 μm bead sets,
111 were comparable between platforms. However, the calculated values revealed more than a 20%
112 variation from the given value, leading to either an underestimation or an overestimation of the
113 FITC MESF units (Figure 1d). These results show that slight differences in the slope of the
114 calibration lines of the different MESF bead sets become more prominent when extrapolation needs
115 to be extended into the dim area beyond the fluorescence intensities of the calibration beads
116 themselves. Since the same slope differences occurred on all three platforms (Figure 1c), this
117 observation is not related to the type of instrument used (e.g.; digital or analog, photomultiplier
118 (PMT) or avalanche photodiode (APD), jet-in-air or cuvette based). Furthermore, this recurring

119 pattern on all platforms makes it unlikely that differences in slopes were caused by instrument non-
120 linearity. Further evidence to rule out non-linearity issues is provided by linear plotting of the
121 values, showing no non-linearity issues (Figure S2a-c), and demonstrating instrument linearity on
122 the BD Influx following the approach described by Bagwell et al [9] (Figure S3). Furthermore, we
123 ruled out that slope differences were a result of variations between separate measurements (Figure
124 S4), and confirmed by testing both custom-made and commercial FITC MESF beads (Figure S1)
125 and FITC MESF beads and PE MESF beads (Figure S2 d-f) that slope variability is inherent to the
126 use of calibrator beads.

127 **MESF assignments of FITC fluorescence intensities to synthetic silica nanoparticles depend** 128 **on the MESF-bead calibrator set**

129 We next investigated how calibration with the two FITC MESF bead sets of 6 μm and 2 μm impacts
130 fluorescent assignment to dim fluorescent nanoparticles. For this purpose 550 nm silica NPs
131 containing 6 populations with FITC fluorescence intensities below or within the range of the
132 calibration beads were measured on the BD Influx. Singlets were gated (Figure S5) and an
133 histogram overlay was generated showing 6 different FITC fluorescence intensities (Figure 2a,
134 left). Histograms showing the calibrated FITC MESF units of these silica NPs based on
135 fluorescence calibration with either the 6 μm or 2 μm FITC MESF calibrator bead set are displayed
136 in Figure 2a (respectively middle or right). The obtained MFI and CV values for each silica NP
137 population, as well as the calculated FITC MESF values based on the two calibrator sets are shown
138 in Figure 2b. The calculated FITC MESF values for the silica NPs appeared consistently lower
139 when the regression line of the 6 μm calibration bead sets was used (Figure 2b). This phenomenon
140 is not limited to the use of FITC MESF beads and can solely be explained by the difference in the
141 slope of the regression line of the two calibrator bead sets, as was confirmed by calculating the
142 fluorescent intensity in terms of PE ERF for 200 nm broad spectrum fluorescent polystyrene NPs

143 based on the 6 μm and 2 μm PE MESF calibrator bead sets (Figure S6a). Importantly, multi-
144 intensity peak analysis of the silica NPs revealed that the difference in FITC MESF values of these
145 NPs obtained by the two calibrator bead sets increased in the dimmer range of the fluorescence,
146 with 27.3% variation for the brightest fluorescent peak (p6) to 76.5% variation for the dimmest
147 population of these NPs (Figure 2b). Also the PE ERF values calculated for the relatively dim 200
148 nm broad spectrum fluorescent polystyrene NPs based on the 6 μm or 2 μm PE MESF calibrator
149 bead sets showed a variation of 41.3% (Figure S6a). These results can be explained by the fact that
150 the differences in calculated values increase by extrapolation into the dim area as a consequence of
151 the differences in the slopes of the regression lines between the calibrator bead sets.

152 **MESF calibration using different bead sets leads to variable ERF and MESF values assigned**
153 **to fluorescently CFSE stained and CD9 labeled extracellular vesicles**

154 We next demonstrate the impact of the assignment of FITC ERF units and PE MESF units to a
155 biological EV sample measured on BD Influx by using the four different MESF calibrator sets, i.e.
156 6 and 2 μm FITC MESF and the 6 and 2 μm PE MESF beads. Since the light scatter of these EVs
157 was too low to resolve the EV population from the background signals, fluorescence thresholding
158 was applied [10] based on the CFSE luminal dye staining. Furthermore, the expression of CD9, a
159 tetraspanin enriched on the surface of the 4T1-derived EVs, was analyzed by using a CD9-PE
160 antibody (Figure 3a). Unstained EVs and CFSE stained EVs with a matching isotype-PE control
161 were measured side-by-side (Figure 3a) and fluorescent polystyrene spike-in beads (200 nm) were
162 added to EV samples to determine the EV-concentration and define the EV-gating (Figure S7a).
163 In Figure 3c-d, the histogram overlays show how the fluorescence intensities of the calibrators
164 relate to the fluorescent signals generated by CFSE stained and CD9-PE labeled EVs. Our
165 calibration results revealed a 76.6% variation in the calculated CFSE ERF units on CFSE stained
166 EV and a 156.9% variation in the calculated PE MESF units on CD9-PE labeled EVs when the

167 different MESF calibrator sets were used (Figure 3a-b). Moreover, the fluorescent threshold value
168 of 0.67 used on the BD Influx corresponds to an equivalent of 150 FITC MESF based on the 6 μm
169 beads or 300 FITC MESF based on the 2 μm beads (Figure 3a), which also shows the variation
170 between two bead sets when reporting the level of detection in standardized units.

171

172 **Discussion**

173 The field of small particle flow cytometry is rapidly evolving, where the definition of what and
174 how much can be detected is crucial. Besides the inter-comparability of data, the use of MESF/ERF
175 values generates awareness about the range of fluorescence intensities that can be expected for
176 small particles, such as EVs, and allows to indicate instrument detection sensitivity and to report
177 fluorescence thresholding in calibrated units [8, 11].

178 In line with previous findings, we here showed that linear regression curves derived from
179 calibration beads developed for calibration of fluorescence on cells, can be used to calculate
180 MESF/ERF values for dim NPs and EVs, allowing data inter-comparability with acceptable
181 precision when the same calibrator is used [11]. Since earlier reports pointed out towards
182 variabilities in MESF/ERF assignments between manufacturer's [5], we used different calibrator
183 bead sets from the same manufacturer, assigned by using the same method and internal NIST
184 traceable calibrator and prepared by following the same manufacturing process. Nevertheless, we
185 found that the robustness of a calculated MESF/ERF value varies upon the use of different
186 calibrator bead sets.

187 We here demonstrate that the calibration of dim NPs and EVs is substantially affected by the
188 intrinsic variation within the assignment of MESF/ERF values to the calibrator beads [12]. Since
189 the fluorescent intensities of EVs, based on generic staining and/or on antibody labeling, are far

190 dimmer than the available calibrators calculation of their MESF/ERF values relies on extrapolation
191 of the regression line of the calibrator beads into the dim area. Our data demonstrate that regression
192 lines of different calibrator sets result in different calculated MESF/ERF values for NPs and EVs
193 that have fluorescent intensities at the lower end or below the intensities of the calibrator beads
194 themselves. Due to the increased separation of regression lines with slightly different slopes at the
195 lower end, increasing uncertainties exist in the MESF/ERF assignment for dim NPs and EVs, which
196 compromise the accuracy of the MESF/ERF assignment. Importantly, most available calibrator
197 bead sets do not provide uncertainty values around the given MESF/ERF units, which would help
198 to create awareness about the possibilities and limitations related to MESF/ERF unit reporting.
199 Based on our findings, the use of the same calibrator bead set and the same number of data points
200 of the calibrators used for linear regression would increase robustness of the calculation of
201 MESF/ERF values for inter-laboratory and inter-platform comparison, and detailed description of
202 calibration materials and calculation of MESF/ERF values would increase reproducibility.

203 Clearly, a calibrator with MESF/ERF values closer to the range of fluorescence intensities of the
204 sample of interest and with a low uncertainty of assignment is preferable. Importantly, novel state-
205 of-the-art flow cytometers that are designed to measure small particles rely obligately on sub-
206 micron sized beads to perform MESF/ERF calibration. These state-of-the-art platforms cannot
207 measure the ‘standard’ 6 μm MESF beads [13]. Therefore, there is an urgent need for calibration
208 beads that are validated for small particle flow cytometry.

209 In summary, our results confirm that fluorescence calibration enables data comparison and
210 provides information on the detection sensitivity of the instrument in standardized units [14, 15],
211 but also urge for awareness of the limitations when fluorescence calibration is being employed for
212 EVs and NPs, especially in terms of accuracy. Lastly, for robust assignments of fluorescence values

213 to NPs and EVs, there is a need for multi-institutional collaborations (between research labs,
214 companies and metrology institutions, such as NIST) to produce and validate calibration materials
215 that have low and well-characterized uncertainty of assigned fluorescent values, ideally allowing
216 for data interpolation and with a size range that is compatible for all flow cytometer platforms.

217

218 **Material and Methods**

219 **Calibration beads**

220 For calibration of the fluorescence axis in the fluorescein isothiocyanate (FITC) channel we used
221 two different sets of FITC MESF beads (custom-made, 6 μm lot MM2307 #131-10; #131-8; #130-
222 6; #130-5; #130-3 and 2 μm lot MM2307#156; #159.1; #159.2; #122.3, BD Biosciences, San Jose,
223 CA). For calibration of the fluorescence axis in the PE channel, we used two different sets of PE
224 MESF beads (6 μm , commercial QuantiBrite, Catalog No. 340495 lot 62981 and 2 μm , custom
225 made, lot MM2327#153.1; #153.2; #153.4; #153.5; #153.6, BD Biosciences, San Jose, CA).

226 The 6 μm FITC MESF beads were prepared by reacting various concentration of FITC with PMMA
227 Beads (Bangs Labs) in borate buffer at pH 9.2. The 2 μm FITC beads were prepared by reacting
228 various concentrations of FITC-BSA (with a FITC/BSA molar ratio of 2) with 2 μm carboxylic
229 beads (Bangs Labs) using EDC/NHS chemistry. The 2 μm PE beads were made as described above
230 except various concentrations of PE were used with 2 μm carboxylic beads in EDC/NHS chemistry.
231 These beads were analyzed on a BD LSRFortessa™ (BD Biosciences) and their MESF values were
232 assigned by cross-calibration using commercially available MESF beads (Flow Cytometry
233 Standards Corp.). The FITC ERF values were assigned to both 2 μm and 6 μm beads using a
234 specific lot of FITC-FC Bead (BD Biosciences) as a calibrator with known ERF value, which has
235 been assigned by NIST. This provided us with two distinct calibrator bead sets that were produced

236 through the same manufacturing process and assigned using the same instruments and the same
237 internal NIST traceable calibrator to exclude internal processing variations.

238 In addition, we measured commercially available QuantumTM FITC-5 MESF (7 μm , Catalog No.
239 555, lot 14609, Bangs Laboratories) and AccuCheck ERF Reference Particles Kit (3 μm , Catalog
240 No. A55950, lot #081220207, #081220203, #081220208, Thermo Fisher) which were prepared
241 according to the manufacturer's instructions.

242 All calibration bead sets were measured with gain or voltage settings as would be used for the
243 analysis of small particles (i.e. EVs). In addition, not all beads could be measured on every
244 instrument. For fair cross-platform comparison of the slopes of the regression lines, only the bead
245 populations that could be measured on all instruments were included for linear regression analysis.

246 **Flow cytometer platforms**

247 In this study three flow cytometers were used. A jet in air-based BD Influx (BD Biosciences, San
248 Jose, CA), a BC CytoFLEX LX (Beckman Coulter, Brea, CA) with a cuvette-based system and a
249 cuvette-based SORP BD FACSCelestaTM (BD Biosciences, San Jose, CA) equipped with a
250 prototype small particle side scatter module.

251 The BD Influx flow cytometer was modified and optimized for detection of submicron-sized
252 particles [10]. In brief, FITC was excited with a 488 nm laser (Sapphire, Coherent 200 mW) and
253 fluorescence was collected through a 530/40 bandpass filter. PE was excited with a 562 nm laser
254 (Jive, Cobolt 150 mW) and fluorescence was collected through a 585/42 bandpass filter. Optical
255 configuration of the forward scatter detector was adapted by mounting a smaller pinhole and an
256 enlarged obscuration bar in order to reduce optical background. This reduced wide-angle FSC
257 (rwFSC) allowed detection of sub-micron particles above the background based on forward scatter
258 [10, 16]. Upon acquisition, all scatter and fluorescence parameters were set to a logarithmic scale.

259 To minimize day to day variations, the BD Influx was standardized at the beginning of each

260 experiment by running 100 and 200 nm yellow-green (505/515) FluoSphere beads (Invitrogen,
261 F8803 and F8848). The instrument was aligned until predefined MFI and scatter intensities were
262 reached with the smallest possible coefficient of variation (CV) for rwFSC, SSC and fluorescence.
263 After optimal alignment, PMT settings required no or minimal day to day adjustment and ensured
264 that each measurement was comparable. MESF beads and NPs were measured with a FSC
265 threshold set at 1.0 while for biological EVs a fluorescence threshold was set at 0.67 by allowing
266 an event rate of 10-20 events/second while running a clean PBS control sample.

267 When performing quantitative and qualitative analysis of synthetic NPs and biological EVs,
268 preparations were diluted in PBS as indicated. Upon loading on the Influx, the sample was boosted
269 into the flow cytometer until events appeared, after which the system was allowed to stabilize for
270 30 seconds. Measurements were performed either by a fixed 30 second time or by setting a gate
271 around the spike-in beads and allowing to record a defined number of events in the gate (80 000
272 events) using BD FACS Software 1.01.654 (BD Biosciences).

273 The CytoFLEX LX was used without any tailor-made modifications in the configuration. Before
274 measurements, the manufacturer recommended startup and QC procedure were run first. All scatter
275 and fluorescence parameters were set to a logarithmic scale. FITC was measured with a 50 mW
276 488 nm laser and fluorescence was measured through a 525/40 band pass filter at gain 1.0. FITC
277 MESF beads were recorded with an FSC threshold at 1000. Measurements were performed using
278 CytExpert 2.1 (Beckman Coulter).

279 The SORP BD FACSCelesta™ was equipped with a prototype small particle SSC module for
280 improved scatter detection. Before measurement, the recommended CS&T performance check was
281 run to monitor performance on a daily basis and to optimize laser delay. All scatter and fluorescence
282 parameters were set to a logarithmic scale. 100 nm yellow-green (505/515) FluoSphere beads
283 (Invitrogen, F8803) were acquired and used to set optimal fluorescence (FITC detector) PMT-V

284 values. FITC was measured with a 100 mW 488 nm laser through a 530/30 band pass filter. FITC-
285 MESF beads were recorded with an SSC threshold at 200. Measurements were performed using
286 BD FACSDiva™ Software v8.0.3 (BD Biosciences).

287 Further descriptions of each instrument and methods are provided in Data S1 (MiFlowCyt
288 checklist) and Data S2 (MiFlowCyt-EV framework).

289 **Preparation of FITC-doped silica nanoparticles**

290 Synthetic silica nanoparticles (SiNPs) of 550 nm diameter with six different FITC fluorescence
291 intensities were produced by using a modified method of literature reports [17-19]. Briefly, the
292 amine reactive FITC molecules were covalently linked to the silane coupling agent, (3-
293 aminopropyl)-triethoxysilane (APTES) in anhydrous ethanol. Monodisperse silica seeds of ~90
294 nm prepared by using amino acid as the base catalyst [17, 18] were suspended in a solvent mixture
295 containing ethanol, water and ammonia. Then tetraethyl orthosilicate (TEOS) and different
296 volumes of APTES–FITC solutions were added for growing FITC-doped SiNPs by a modified
297 Stöber method [19, 20]. Upon washing three times with anhydrous ethanol, the FITC-doped SiNPs
298 were reacted with TEOS in the solvent mixture to allow growth of a silica layer. The synthesized
299 SiNPs were washed three times with anhydrous ethanol and stocked in anhydrous ethanol. The
300 diameters of SiNPs were measured by transmission electron microscopy.

301 **Isolation and fluorescent staining of extracellular vesicles for flow cytometric analysis**

302 EV-containing samples were obtained from 4T1 mouse mammary carcinoma cell culture
303 supernatants (ATCC, Manassas, VA) as previously described [16, 21, 22]. EVs were stained with
304 5-(and-6)-Carboxyfluorescein diacetate succinimidyl ester (CFDA-SE, hereinafter referred as
305 CFSE) (Thermo Fisher, Catalog No. C1157) and separated as described previously [10]. Briefly, 2
306 µl of the isolated 4T1 EVs (corresponding to a concentration of 1.44 E12 particles/mL as
307 determined by nanoparticle tracking analysis) were mixed with 18 µl PBS/0.1% aggregate-depleted

308 (ad)BSA. For antibody labeling, samples were first resuspended in 15.5 μ L PBS/0.1% adBSA and
309 incubated with 0.5 μ g of rat anti-mouse CD9-PE (Clone: KMC8, IgG2a, κ , lot 7268877, BD
310 Biosciences) or matched isotype antibodies (Rat IgG2a, κ , PE-conjugated, lot 8096525, BD
311 Biosciences) for 1h at RT while protected from light. EVs were then stained with 40 μ M CFSE in
312 a final volume of 40 μ l. The sealed tube was incubated for 2h at 37°C while protected from light.
313 Next, staining was stopped by adding 260 μ l PBS/0.1% adBSA. After fluorescent staining, EVs
314 were separated from protein aggregates and free reagents by bottom-up density gradient
315 centrifugation in sucrose for 17.30 h at 192,000 g and 4°C using a SW40 rotor (k-factor 144.5;
316 Beckman Coulter, Fullerton, California, USA). Twelve fractions of 1 mL were then collected from
317 the top of the gradient and respective densities were determined by refractometry using an Atago
318 Illuminator (Japan). For analysis by flow cytometry, EV samples corresponding to a 1.14 g/mL
319 density were diluted 1:20 in PBS prior measurement. MIFlowCyt-EV framework [8] were followed
320 whenever applicable (Data S2).

321 **Concentration determination by using spike-in beads**

322 EV concentration was normalized using a spiked-in external standard containing 200 nm orange
323 (540/560) fluorescent beads (Invitrogen, F8809). The concentration of the beads was determined
324 by Flow NanoAnalyzer N30 (NanoFCM, Xiamen, China) and stocked at 5.7E10 particles/mL.
325 Beads were diluted 1:10⁴ in PBS and added to the EV samples, mixed and measured on the flow
326 cytometer. Bead count was used to calculate the EV concentration for BD Influx measurements.

327 **Data analysis**

328 For fluorescence calibration each bead peak population was gated using FlowJo Version 10.5.0
329 and MFI were obtained for further least square linear regression analysis. Data was handled in
330 Microsoft Excel and figures were prepared using GraphPad Prism version 8.0 (GraphPad Software
331 Inc). The software FCMPASS Version v2.17 was used to generate files with calibrated axis units

332 in the histograms and dot plots shown [23] (Software is available on
333 <http://go.cancer.gov/a/y4ZeFtA>).

334 **Data availability**

335 All EV data of our experiments have been submitted to the EV-TRACK knowledgebase (EV-
336 TRACK ID: EV210047) [24]. All flow cytometric data files have been deposited at the Flow
337 Repository (FR-FCM-Z3FJ).

338

339 **Funding Statement**

340 This research is supported by the European Union's Horizon 2020 research and innovation
341 programme under the Marie Skłodowska-Curie grant agreement No 722148 and by the National
342 Natural Science Foundation of China (21934004 and 21627811). E. L. A. is supported by the
343 European Union's Horizon 2020 research and innovation programme under the Marie Skłodowska-
344 Curie grant agreement No 722148.

345

346 **Author Contributions**

347 E.L.A. designed and performed experiments, analyzed data and wrote the manuscript. T.B.
348 performed experiments and gave conceptual advice. L.W. gave technical and conceptual advice.
349 M.M., Y.T. and X.Y. prepared materials and gave technical advice. G.J.A.A. and M.H.M.W.
350 supervised the research, designed (performed) experiments and wrote the manuscript. G.J.A.A. and
351 M.H.M.W. contributed equally as senior author. All authors critically reviewed and edited the
352 manuscript.

353

354 **Acknowledgments**

355 The authors would like to thank Prof. An Hendrix (Laboratory of Experimental Cancer Research,
356 Ghent University, Belgium) for the possibility to prepare and analyze M4T1 derived EV in her lab,
357 Dr. Joshua A. Welsh (National Cancer Institute, Bethesda, MD) for helpful discussion and Ludo
358 Monheim (BD Biosciences, Erembodegem, Belgium) for helpful technical support. FITC-MESF
359 and 2 μm PE-MESF beads were kindly provided by BD Biosciences (prepared by Dr. Majid
360 Mehrpouyan) as part of the European Union's Horizon 2020 research and innovation programme
361 under the Marie Skłodowska-Curie grant agreement No 722148.

362

363 **Declaration of interest disclosure**

364 Tina Van Den Broeck and Majid Mehrpouyan are both employees of BD Biosciences, a business
365 unit of Becton, Dickinson and Company. During the course of this study, the Wauben research
366 group, Utrecht University, Faculty of Veterinary Medicine, Department of Biomolecular Health
367 Sciences and BD Biosciences collaborated as a co-joined partner in the European Union's Horizon
368 2020 research and innovation programme under the Marie Skłodowska-Curie grant agreement No
369 722148. Xiaomei Yan declares competing financial interests as a cofounder of NanoFCM Inc., a
370 company committed to commercializing the nano-flow cytometry (nFCM) technology.

371

372 **Supporting Information**

373 Additional supporting information can be found online in the corresponding section at the end of
374 the article.

375 **Data S1.** Author Checklist: MIFlowCyt-Compliant Items.

376 **Data S2.** MIFlowCyt-EV framework.

377 **Figure S1.** Comparison of the inclusion of different data points into linear regression analysis by
378 using custom-made and commercial FITC MESF bead sets.

379 **Figure S2.** Analysis of different MESF bead sets measured on the BD Influx.

380 **Figure S3.** Analysis of instrument linearity on the BD Influx.

381 **Figure S4.** Evaluation of measurement variability of 2 μm FITC MESF beads measured on the BD
382 Influx.

383 **Figure S5.** Gating strategy for synthetic silica NPs.

384 **Figure S6.** 200 nm fluorescent polystyrene NPs.

385 **Figure S7.** Gating strategy for external spiked-in beads and biological EV samples.

386

387 **ORCID**

388 Estefanía Lozano-Andrés <https://orcid.org/0000-0002-7305-0776>

389 Lili Wang <https://orcid.org/0000-0003-2456-898X>

390 Xiaomei Yan <http://orcid.org/0000-0002-7482-6863>

391 Marca H.M. Wauben <https://orcid.org/0000-0003-0360-0311>

392 Ger. J.A. Arkesteijn <https://orcid.org/0000-0001-7739-582X>

393

394

395

396

397 **References**

- 398 1. Hoffman, R.A., *Standardization, calibration, and control in flow cytometry*. Curr Protoc Cytom, 2005. **Chapter**
399 **1:** p. Unit 1 3.
- 400 2. Wang, L. and R.A. Hoffman, *Standardization, Calibration, and Control in Flow Cytometry*. Curr Protoc Cytom,
401 2017. **79:** p. 1 3 1-1 3 27.
- 402 3. Gaigalas, A.K., et al., *Quantitating Fluorescence Intensity From Fluorophore: Assignment of MESF Values*. J
403 Res Natl Inst Stand Technol, 2005. **110(2):** p. 101-14.
- 404 4. Wang, L., et al., *Quantitating Fluorescence Intensity From Fluorophores: Practical Use of MESF Values*. J Res
405 Natl Inst Stand Technol, 2002. **107(4):** p. 339-53.
- 406 5. Hoffman, R.A., et al., *NIST/ISAC standardization study: variability in assignment of intensity values to*
407 *fluorescence standard beads and in cross calibration of standard beads to hard dyed beads*. Cytometry A,

- 408 2012. **81**(9): p. 785-96.
- 409 6. Nolan, J.P., *Flow Cytometry of Extracellular Vesicles: Potential, Pitfalls, and Prospects*. Curr Protoc Cytom,
410 2015. **73**: p. 13 14 1-16.
- 411 7. Lian, H., et al., *Flow Cytometric Analysis of Nanoscale Biological Particles and Organelles*. Annu Rev Anal
412 Chem (Palo Alto Calif), 2019. **12**(1): p. 389-409.
- 413 8. Welsh, J.A., et al., *MIFlowCyt-EV: a framework for standardized reporting of extracellular vesicle flow*
414 *cytometry experiments*. J Extracell Vesicles, 2020. **9**(1): p. 1713526.
- 415 9. Bagwell, C.B., et al., *A simple and rapid method for determining the linearity of a flow cytometer amplification*
416 *system*. Cytometry, 1989. **10**(6): p. 689-94.
- 417 10. van der Vlist, E.J., et al., *Fluorescent labeling of nano-sized vesicles released by cells and subsequent*
418 *quantitative and qualitative analysis by high-resolution flow cytometry*. Nat Protoc, 2012. **7**(7): p. 1311-26.
- 419 11. Welsh, J.A. and J.C. Jones, *Small Particle Fluorescence and Light Scatter Calibration Using FCMPASS Software*.
420 Curr Protoc Cytom, 2020. **94**(1): p. e79.
- 421 12. Draper, N.R. and H. Smith, *Applied regression analysis*. 1981, New York: Wiley.
- 422 13. Tian, Y., et al., *Protein Profiling and Sizing of Extracellular Vesicles from Colorectal Cancer Patients via Flow*
423 *Cytometry*. ACS Nano, 2018. **12**(1): p. 671-680.
- 424 14. Welsh, J.A., J.C. Jones, and V.A. Tang, *Fluorescence and Light Scatter Calibration Allow Comparisons of Small*
425 *Particle Data in Standard Units across Different Flow Cytometry Platforms and Detector Settings*. Cytometry
426 A, 2020. **97**(6): p. 592-601.
- 427 15. Nolan, J.P. and S.A. Stoner, *A trigger channel threshold artifact in nanoparticle analysis*. Cytometry A, 2013.
428 **83**(3): p. 301-5.
- 429 16. Arkesteijn, G.J.A., et al., *Improved Flow Cytometric Light Scatter Detection of Submicron-Sized Particles by*
430 *Reduction of Optical Background Signals*. Cytometry A, 2020. **97**(6): p. 610-619.
- 431 17. Yokoi, T., et al., *Periodic arrangement of silica nanospheres assisted by amino acids*. J Am Chem Soc, 2006.
432 **128**(42): p. 13664-5.
- 433 18. Yokoi, T., et al., *Mechanism of Formation of Uniform-Sized Silica Nanospheres Catalyzed by Basic Amino Acids*.
434 Chemistry of Materials, 2009. **21**(15): p. 3719-3729.
- 435 19. Stöber, W., A. Fink, and E. Bohn, *Controlled growth of monodisperse silica spheres in the micron size range*.
436 Journal of Colloid and Interface Science, 1968. **26**(1): p. 62-69.
- 437 20. Giesche, H., *Synthesis of monodispersed silica powders II. Controlled growth reaction and continuous*
438 *production process*. Journal of the European Ceramic Society, 1994. **14**(3): p. 205-214.
- 439 21. Vergauwen, G., et al., *Confounding factors of ultrafiltration and protein analysis in extracellular vesicle*
440 *research*. Sci Rep, 2017. **7**(1): p. 2704.
- 441 22. Geeurickx, E., et al., *The generation and use of recombinant extracellular vesicles as biological reference*
442 *material*. Nat Commun, 2019. **10**(1): p. 3288.
- 443 23. Welsh, J.A., et al., *FCMPASS Software Aids Extracellular Vesicle Light Scatter Standardization*. Cytometry A,
444 2019.
- 445 24. Consortium, E.-T., et al., *EV-TRACK: transparent reporting and centralizing knowledge in extracellular vesicle*
446 *research*. Nat Methods, 2017. **14**(3): p. 228-232.

447 448 **Main figure legends**

449 **Figure 1. Evaluation of two different FITC MESF bead sets for the calibration of fluorescent**
450 **intensities across three flow cytometer platforms. (a)** Histogram overlays (axis in arbitrary units)
451 of FITC fluorescent intensity peaks derived from the 6 μm (upper row) or the 2 μm (lower row)
452 FITC MESF beads **(b)** Table showing the median fluorescence intensity (MFI) statistic derived
453 from each of the fluorescent intensity peaks from dimmer to brighter being expressed in arbitrary

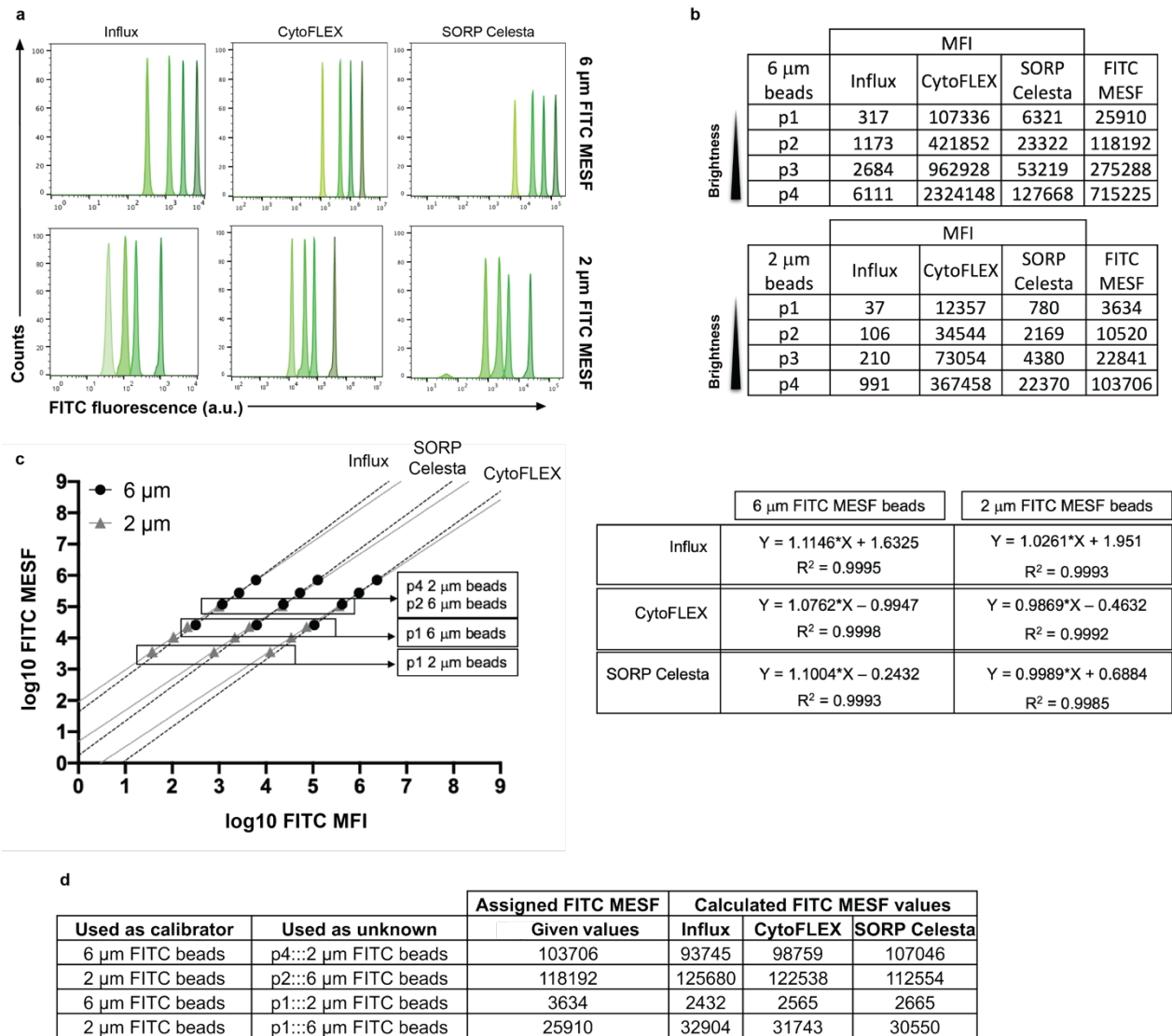
454 units as well as the assigned MESF values (right column). **(c)** Least square linear regression
455 analysis of 6 μm (black circles) and 2 μm (grey triangles) FITC MESF beads. Provided FITC
456 MESF and measured FITC MFI values were transformed to log and plotted in a log-log fashion for
457 the three platforms. **(d)** Table indicating the expected and calculated FITC MESF values for each
458 sample used in the analysis.

459
460 **Figure 2. MESF bead-based calibration of fluorescence signals from synthetic silica NPs. (a)**
461 Histogram overlay showing FITC fluorescence in arbitrary units (a.u.) (left), FITC MESF
462 calibrated axis based on the 6 μm (middle) and 2 μm FITC MESF beads (right) from the six
463 differently FITC-labeled 550 nm NP gated populations. **(b)** Table showing the MFI and CV as well
464 as the calculated FITC MESF values for each of the unknown populations with the percentage of
465 variation between the two calculated reference values.

466
467 **Figure 3. MESF bead-based calibration of fluorescent signals from biological EV samples.**
468 **(a)** Analysis of EV samples by using a fluorescence threshold. Unstained EVs control (left), CFSE
469 and isotype-PE stained EVs (middle) and CFSE and CD9-PE stained EVs (right) dot plots showing
470 CFSE fluorescence Vs PE fluorescence in arbitrary units (a.u.) (upper row) or CFSE ERF Vs PE
471 MESF calibrated axis based on either the 6 μm (middle row) or 2 μm calibration beads (lower
472 row). The dashed line in each dot plot indicates the fluorescence threshold value used. Number of
473 events within the EV gate and MFI values for either CFSE or PE fluorescence (a.u.) are indicated
474 in the top row. CFSE ERF and PE MESF values are indicated based on the 6 μm (middle row) or
475 2 μm beads (lower row). **(b)** Table showing the ERF or MESF values obtained after calibration for
476 the CFSE and CD9-PE stained EVs and the percentage of variation between the use of the 6 μm or
477 2 μm bead sets. **(c)** Histogram overlays displaying fluorescence in arbitrary units from CFSE

478 stained EVs (blue) next to the 6 μm or 2 μm FITC-MESF bead set (green). **(d)** Histogram overlays
 479 displaying fluorescence in arbitrary units from CD9-PE labeled EVs (purple) next to the 6 μm or
 480 2 μm PE-MESF bead set (red).

481 **Figure 1**



482

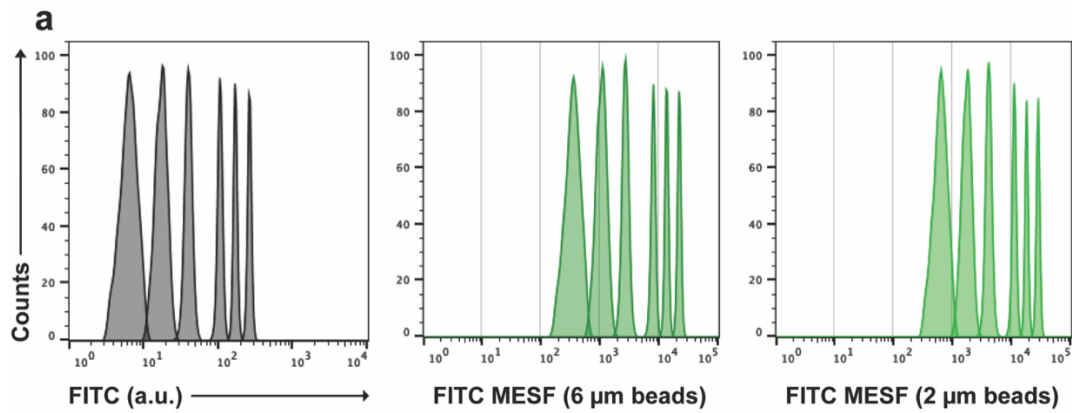
483

484

485

486

487 **Figure 2**

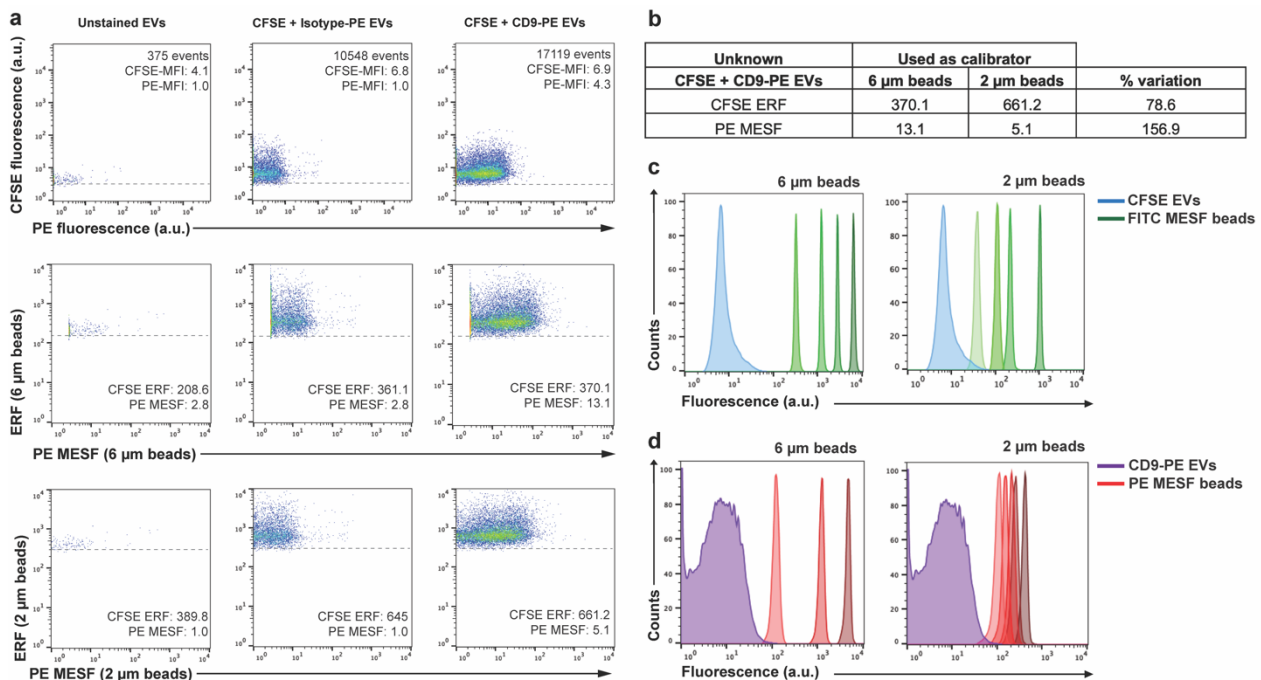


b

Unknown	MFI	CV	Calculated FITC MESF values		
			Used as calibrator		
			6 μm FITC beads	2 μm FITC beads	% variation
p1	6.35	25.53	337	595	76.5
p2	17.20	17.83	1022	1654	61.8
p3	39.60	10.89	2590	3894	50.3
p4	104.90	6.86	7671	10581	37.9
p5	167.00	5.12	12881	17050	32.4
p6	258.90	5.10	20995	26734	27.3

488

489 **Figure 3**



490